Electronic surface states on (110) aluminum*

Ed Caruthers, Leonard Kleinman, and Gerald P. Alldredge
Department of Physics, University of Texas, Austin, Texas 78712
(Received 8 October 1973)

We have calculated the projection of the three-dimensional energy bands of aluminum onto the two-dimensional Brillouin zone (BZ) of the (110) face. Using a pseudopotential constructed in the same way as that in our publication on the (001) face, we have calculated eigenvalues and eigenfunctions at high-symmetry points of the two-dimensional BZ for (110) thin films. Contrary to the results of Boudreaux, who found no (110) surface states, we find that surface states exist in the energy gaps of the projected bands at all high-symmetry points ($\bar{\Gamma}$, $\bar{Y}$, $\bar{S}$, and $\bar{X}$) of the two-dimensional BZ.

In this paper using methods we have previously reported,[1,2] we calculate the projection of the three-dimensional energy bands of aluminum onto the two-dimensional Brillouin zone (BZ) of the (110) face and calculate eigenvalues and eigenfunctions at high-symmetry points of the two-dimensional BZ for thin (110) aluminum films. Because of the lower symmetry of the (110) film we were not able to calculate the energy bands along symmetry lines as we did for the (001) film.[2] However, unless one is specifically interested in *very* thin films, the projection gives all the information one needs except for the existence of surface states. We are especially interested in the (110) surface because Boudreaux[3] has claimed that although surface states exist on the (001) and (111) surfaces, they do not exist on the (110) surface of aluminum. The thin-film calculations at the $\bar{\Gamma}$, $\bar{Y}$, $\bar{X}$, and $\bar{S}$ symmetry points which we present here, demonstrate beyond any doubt that surface-state bands exist within all the energy gaps of the (110) projected energy bands.

Figure 1 shows the (110) face of the fcc structure. The atoms are rectangularly arranged in alternating layers equally separated by $a/2\sqrt{2}$. The unit cell for a film will have the thickness of the film including the selvage, and will have planar dimensions as shown by the dashed lines in Fig. 1. Atoms in A layers are always in the centers of unit cells, and atoms in B layers are always on the edges of the unit cells. The total number of atoms in the unit cell will be equal to the number of layers in the film. For our thin-film calculations we use an odd number of layers so that the film has reflection symmetry through the central A layer.

Figure 2 superposes the BZ for the (110) face on the BZ for the fcc structure. The dashed lines show a cross section of the three-dimensional (3D) zone through Γ and perpendicular to the [110] direction. The dotted lines show the way in which the hexagonal and square faces of the 3D zone appear when viewed from the [110] direction. Our notation for the high-symmetry points is the same as that which has been previously used in studies of surface vibrational modes.[4a]

As in Ref. 2 (hereafter called I) we map the basic structure of the two-dimensional bands from the three-dimensional bands. The slab-adapted 3D Brillouin zone compatible with the 2D BZ has the same base as the 2D BZ and extends in the third dimension between $\pm(2\pi/a)(\frac{1}{2},\frac{1}{2},0)$. To find the projected bands at the point $\bar{k}=(2\pi/a)(k_x,k_y)$ we calculate the three-dimensional energy bands along the line $k_x(2\pi/a)(\bar{1},1,0)+k_y(2\pi/a)(0,0,1)+k_z(2\pi/a)(1,1,0)$ for fixed k_x and k_y and $0\leq k_z\leq 1$.[4b] Because of the reflection symmetry in the central

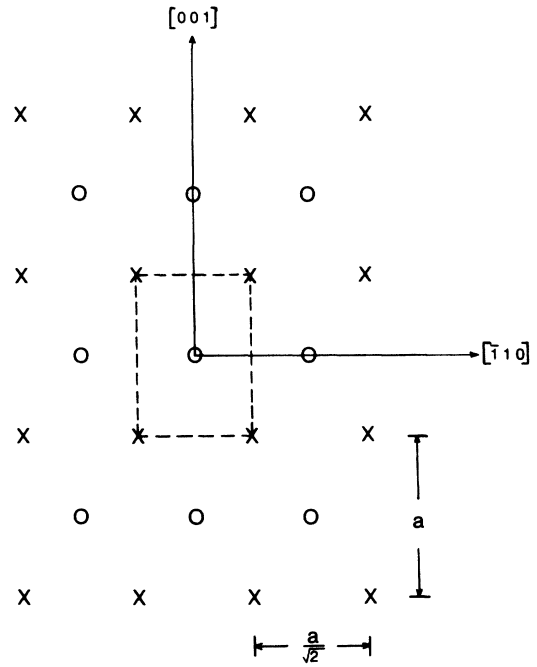

FIG. 1. Crystal structure for a (110) film of fcc aluminum. Circles denote atoms in A layers; crosses denote atoms in B layers; dashed lines show the unit cell. Lengths of the sides of the unit cell are given in terms of a = 4.04 Å, the edge length for the aluminum face-centered cube.

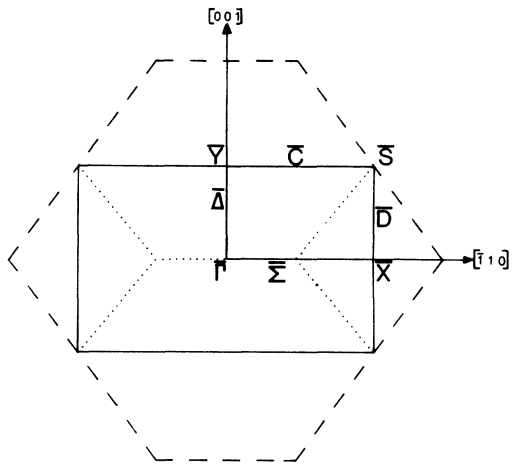

FIG. 2. Brillouin zone for a (110) fcc aluminum film, and perspective view of the three-dimensional BZ.

plane, states with k_z's in the lower-half of the extended-slab-adapted BZ are degenerate with those in the upper-half.

Figure 3 shows the main features of the projection. Crosshatching denotes a continuum of states of a given two-dimensional symmetry. Since these are projected from bulk states, surface localized electronic states can exist only for values of $\bar{k}$ and for energies at which gaps exist in the projected bands. We therefore concentrate our attention on the origin of these gaps.

The $\bar{\Gamma}$ eigenvalues are projected from the 3D bands[5] along the line from Γ to K to X. There are two types of symmetry in $\bar{\Gamma}$ states, arising from the Σ_1 and Σ_3 states in 3D. Thus, even though there is no absolute gap at $\bar{\Gamma}$, there is a gap in the $\bar{\Gamma}_1$ subband arising from the gap in Σ_1 states between -0.362 Ry at $k_z = 0.76$ and -0.391 Ry at $k_z = 0.78$. Surface states of symmetry $\bar{\Gamma}_1$ may therefore exist in the energy range $-0.391 \leq E_{s.s.} \leq -0.362$ Ry. But because there is a continuum of $\bar{\Gamma}_3$ states from -0.555 Ry up to positive energies, no $\bar{\Gamma}_3$ surface states are possible. $\bar{\Gamma}_1$ states are even with respect to reflections through the $\bar{x}$ and $\bar{y}$ axes, while $\bar{\Gamma}_3$ states are even with respect to reflection through $\bar{y}$ and odd with respect to reflection through $\bar{x}$. Therefore along the $\bar{\Delta}$ line from $\bar{\Gamma}$ to $\bar{Y}$, both $\bar{\Gamma}_1$ and $\bar{\Gamma}_3$ states connect to $\bar{\Delta}_1$ states which are even with respect to reflection through $\bar{y}$. Hence, the $\bar{\Gamma}_1$ subband gap does not persist along $\bar{\Delta}$. The eigenvalues along $\bar{\Delta}$ are calculated from the 3D points $(2\pi/a)(k_x, k_z, \alpha)$, $0 \leq \alpha \leq \frac{1}{2}$ and $0 \leq k_z \leq 1$ and are not degenerate. But at $\bar{Y}$, pairs of $\bar{\Delta}_1$ states arising from $k_z = \beta$ and $k_z = 1 - \beta$ become degenerate (except for $\beta = \frac{1}{2}$). The gap at $\bar{Y}$ arises from repulsion of $k_z = \frac{1}{2}$ states by V_{111}. In 3D this is just the L-point gap $(\frac{1}{2}, \frac{1}{2}, \frac{1}{2})$. This gap persists as we go from $\bar{Y}$ toward $\bar{\Gamma}$ as a locus of points at which lines of the same k_z repel one another (for $0.5 \leq k_z \leq 0.733$). But the gap narrows and finally pinches off at $\bar{\Gamma}$ where, for $E = -0.454$ Ry, $\bar{\Gamma}_1$ and $\bar{\Gamma}_3$ states are degenerate. This degeneracy arises from the crossing, in 3D, of the Σ_1 and Σ_3 bands at $k_z = 0.733$. That is, the gap along $\bar{\Delta}$ is due to the repulsion of the two lowest bands in 3D. Along Σ these have different symmetries and cross, so that the $\bar{\Delta}$ gap pinches off as we approach $\bar{\Gamma}$.

The $\bar{Y}$ gap also persists along the $\bar{C}$ direction, defined by the 3D points $(2\pi/a)(k_x - \alpha, k_z + \alpha, \frac{1}{2})$, $0 \leq \alpha \leq \frac{1}{2}$, $0 \leq k_z \leq 1$. The $\bar{Y}$ degeneracy also persists between $k_z = \beta$ and $k_z = 1 - \beta$.[6] The $\bar{Y}$ gap persists between $k_z = \frac{1}{2}$ states for about 75% of the way from $\bar{Y}$ to $\bar{S}$. Then it is crossed by lines with values of

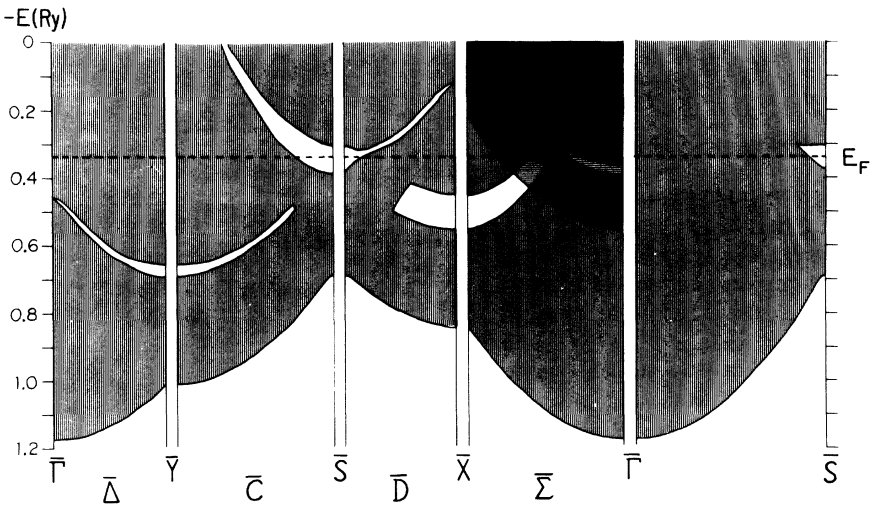

FIG. 3. Two-dimensional projection of the three-dimensional energy bands onto the (110) face. $E_F = -0.33$ Ry.

k_z less than $\frac{1}{2}$. At $\bar{S}$ there is a band gap between -0.303 and -0.382 Ry which comes from $k_z=\frac{1}{2}$ and the 3D W point, $(0,1,\frac{1}{2})$. This gap persists in the $\bar{C}$ direction as a locus of points at which lines of same k_z repel each other. The gap crosses the Fermi level and reaches positive energies about 70% of the way toward $\bar{Y}$.

The $\bar{S}$ gap also extends in the $\bar{D}$ direction, defined by $(2\pi/a)(k_z-\frac{1}{2},\ k_z+\frac{1}{2},\alpha)$, $\frac{1}{2}\geq\alpha\geq 0$, $0\leq k_z\leq 1$. All states along $\bar{D}$ are degenerate pairs,[7] but at $\bar{X}$ there are both $\bar{X}_1$, $\bar{X}_4$ degenerate pairs with energy greater than -0.84 Ry and $\bar{X}_2$, $\bar{X}_3$ pairs with energy greater than -0.21 Ry. The $\bar{S}$ gap persists in the $\bar{D}$ direction as a locus of points where lines of the same k_z repel one another, k_z decreasing from 0.50 to 0.27. At the $\bar{X}$ point the gap is pinched off by a quadruple degeneracy. At $k_z=0.27$ and $E=-0.116$ Ry, $\bar{X}_1$, $\bar{X}_4$ and $\bar{X}_2$, $\bar{X}_3$ are all degenerate. Lower down at $\bar{X}$, there is a gap from -0.450 to -0.550 Ry in the $\bar{X}_1$, $\bar{X}_4$ continuum. This arises from $k_z=\frac{1}{2}$ and the X point in 3D, $(0,1,0)$. It extends toward $\bar{S}$ as a gap between $k_z=\frac{1}{2}$ eigenvalues. But about halfway along $\bar{D}$ it starts being crossed by states of different k_z.

From $\bar{X}$, $\bar{X}_1$ and $\bar{X}_4$ states connect to $\bar{\Sigma}_1$ states, which connect to $\bar{\Gamma}_1$ states, and $\bar{X}_2$ and $\bar{X}_3$ states both connect to $\bar{\Sigma}_3$ states which connect to $\bar{\Gamma}_3$ states. The $\bar{\Sigma}_3$ states form a continuum whose extent is indicated by horizontal crosshatching. There are no gaps in the $\bar{\Sigma}_3$ subband. But the gap at $\bar{X}$ persists in the $\bar{\Sigma}_1$ states as a locus of points where lines of the same k_z repel each other. It is crossed about $\frac{1}{3}$ of the way to $\bar{\Gamma}$ by $\bar{\Sigma}_3$ states, but it persists as a subband gap until $\bar{\Sigma}_1$ states of different k_z start to cross. This does not quite connect to the subband gap which propagates from the $\bar{\Gamma}_1$ gap mentioned above.

Since $E_F=-0.33$ Ry is within the $\bar{S}$ gap, it is possible that surface states may exist which are below E_F at $\bar{S}$ and which cross the Fermi level as they go away from $\bar{S}$. These would be current-carrying surface states and would introduce bulk-to-surface conductivity differences. We therefore include the shape of the $\bar{S}$ gap as it propagates along the line to $\bar{\Gamma}$. In this direction of no planar symmetry the gap pinches off more rapidly than along high symmetry directions.

The projection in Fig. 3 shows where gaps can exist in a thin film. In the limit of very thick films, solutions must go over to the bulk solutions, so that gap edges will be exactly as projected. But for films less than about 100 Å thick the gaps are usually wider, and are typically displaced downward somewhat. For a thick film, surface states will occur in degenerate pairs, even and odd with respect to reflection in the central plane of atoms. But for a thin film the degeneracy will be somewhat split. The only way to be certain whether a given band gap contains a surface state is to perform an eigenvalue calculation, and then plot the wave functions.

In comparison to the (001) face of aluminum,[2] the (110) face has rectangular rather than square planar symmetry. This means that convergence of the eigenvalue calculations requires more planar-symmetrized combinations of plane waves (S2DPWs).[1] For this reason we perform eigenvalue calculations only at the high-symmetry points $\bar{\Gamma}$, $\bar{X}$, $\bar{S}$, and $\bar{Y}$. The (110) face also differs from the (001) face in distance between adjacent layers: $a/2\sqrt{2}$ for (110) vs $\frac{1}{2}a$ for the (001). This means that for films of the same thickness as these used in our study on the (001) face, we must have more layers. Our thin-film potential is derived as in I. Figure 4 shows the $\bar{G}=0$ Fourier transform of our potential for a film of 19 occupied layers and 4 selvage layers on each side. All other transforms of the potential come from a simple overlap of Heine-type atomic pseudopotentials.[8] For the $\bar{G}=0$ transform we combined overlapped pseudopotentials with the Lang-Kohn jellium potential.[9] For this potential, we expect convergence of the $\bar{\Gamma}$ eigenvalues to require 6 S2DPWs, and 30 values each of $k_3^{\pm}$ for $\sin(k_3^{-}z)$ and $\cos(k_3^{+}a)$ as basis functions in the [110] direction.[1] We have tested planar convergence by comparing eigenvalues with those resulting from nine S2DPWs and 30 sines and cosines, and found that no eigenvalue changes by

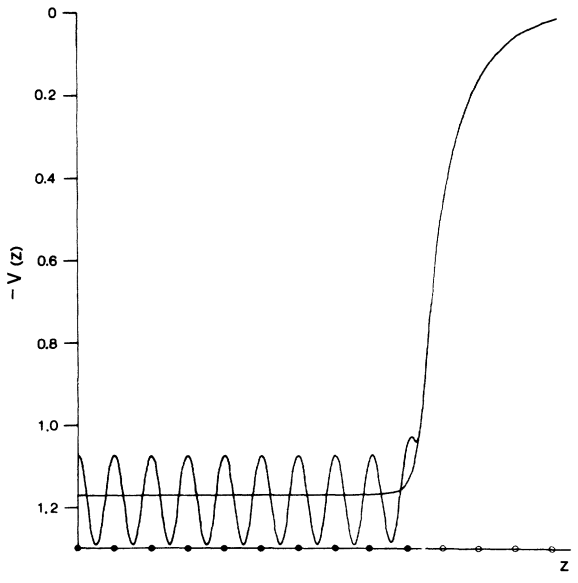

FIG. 4. The $\bar{G}=0$ Fourier transform of the pseudopotential used for a 19-layer film with four selvage layers on each side. Also included is the Lang-Kohn potential (Ref. 6) for jellium with the appropriate electron density. Closed circles denote occupied layers and open circles denote unoccupied selvage layers.

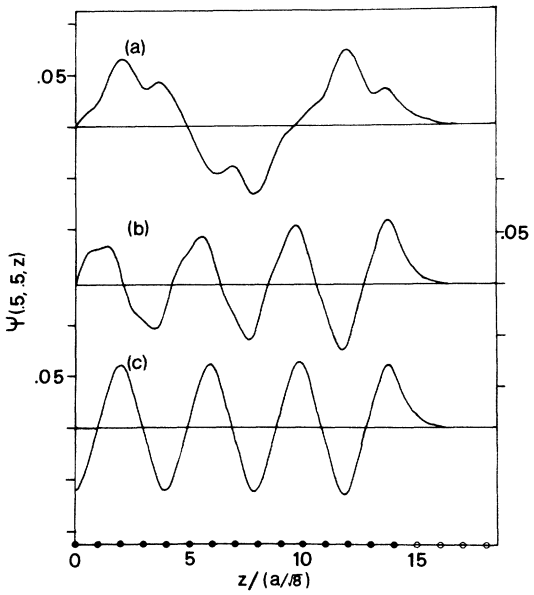

FIG. 5. Surface states through the corner of the two-dimensional unit cell for a (110) aluminum film of 29 occupied layers and four selvage layers on each side. (a) $\bar{\Gamma}_1^-$ wave function. (b) $\bar{Y}_3^-$ wave function well centered in its energy gap. (c) $\bar{Y}_3^+$ wave function at the top of its energy gap.

more than 0.0011 Ry. We have tested convergence in the third direction by comparing to eigenvalues derived from six S2DPWs and 46 values each of $k_3^\pm$ for $\sin(k_3^- z)$ and $\cos(k_3^+ z)$, and no eigenvalue changes by more than 0.0025 Ry.

In Figs. 5 and 6 we present pseudo-wave-functions for the surface states at each of the four high-symmetry points in the BZ. At each point we have worked with the thickest possible film in order to see the falloff of the wave functions as clearly as possible. At $\bar{\Gamma}$ and $\bar{Y}$ we performed our calculations on films with 29 occupied layers (41.5 Å thick) and four selvage layers on either side. At $\bar{X}$ and $\bar{S}$ we could only work with 19 occupied layers (27.2 Å thick) and four selvage layers on each side. A curious feature of this calculation was that at all four points, a surface state of odd reflection symmetry was well centered in gap, while its partner of even symmetry was nearer the top or bottom of the gap. At high-symmetry points in the (001)-face BZ we found[2] that the surface states lay symmetrically about the center of the band gap. Since the decay constant increases with distance from the band edge[10] one sees very different decay constants for $\bar{Y}_3^-$ and $\bar{Y}_3^+$ surface states. This makes it impossible for us to say what the decay constants would be in thick films where, e. g., the $\bar{Y}_3^+$ and $\bar{Y}_3^-$ eigenvalues must become degenerate. This also makes it difficult to correlate decay constants with gap widths. The decay constants of the odd-parity surface states in the $\bar{\Gamma}$, $\bar{Y}$, and $\bar{S}$ gaps seem to increase with gap widths, but the $\bar{X}_1^-$ surface state does not decay more rapidly than the $\bar{S}_1^-$ surface state. Note that the Y_3^+ wave function is much smoother than the Y_3^-. These functions which are plotted for $\bar{r} = (\frac{1}{2}\sqrt{2}, 1)a/2$ go through atoms in the B planes. They would like to have nodes near the B planes in order to avoid the repulsive pseudopotential in the atomic cores but the Y_3^- function is required (because of its antisymmetry about the central plane) to have a node in the central A plane. Therefore, it is large at the B planes in the region of the center of the film.

We have found surface states at all four high-symmetry points of the (110)-A1 two-dimensional BZ. Except for the $\bar{\Gamma}$ surface states which extend only in the $\bar{\Sigma}$ direction, these surface states exist in large areas of the 2D BZ around the symmetry points. Since the $\bar{S}_1^\pm$ surface states have eigenvalues of -0.374 and -0.36 Ry we expect the degenerate $\bar{S}_1^\pm$ surface states in a thicker film to lie at least 0.03 Ry below the Fermi energy and to cross the Fermi level in the neighborhood of $\bar{S}$. This Fermi line (i. e., two-dimensional Fermi surface) is, in principle, capable of detection by the two-dimensional de Haas–van Alphen effect.[11] We note again that our calculations contradict Boudreaux[3] who reported no surface states exist on the (110) surface of aluminum. He used a model potential which was discontinuous at the crystal surface, but we do not believe that this can be the cause of his negative result.

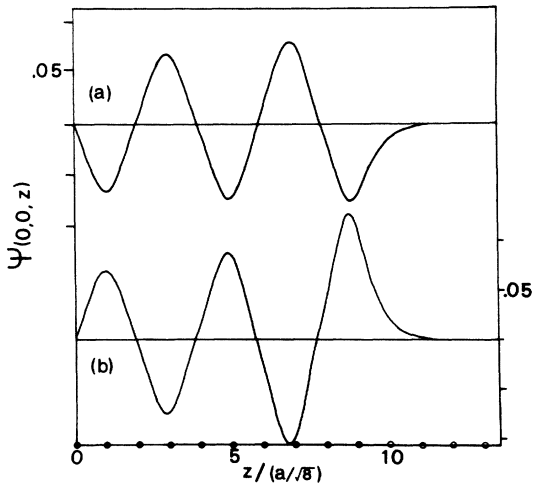

FIG. 6. Surface states through the center of the two-dimensional unit cell for a (110) aluminum film of 19 occupied layers and four selvage layers on each side. (a) $\bar{X}_1^-$ wave function. (b) $\bar{S}_1^-$ wave function.

*Research supported by the Air Force Office of Scientific Research under Grant No. AF-AFOSR-72-2308 and by the National Science Foundation under Grant No. GH-40371.

[1]G. P. Alldredge and L. Kleinman, Phys. Rev. Lett. 28, 1264 (1972).

[2]E. B. Caruthers, L. Kleinman, and G. P. Alldredge, Phys. Rev. B 8, 4570 (1973).

[3]D. S. Boudreaux, Surf. Sci. 28, 344 (1971).

[4](a) R. E. Allen, G. P. Alldredge, and F. W. de Wette, Phys. Rev. B 4, 1661 (1971). (b) Since the slab-adapted unit cell is larger than the primitive unit cell, the slab-adapted BZ is smaller than the primitive BZ. In order to contain all the points in the primitive BZ one must use an extended-slab BZ which is obtained by repeating the slab-adapted BZ in the surface-normal direction until the surface-normal faces of the BZ are separated by a 3D reciprocal-lattice vector, which in this case is $(2\pi/a)(2,2,0)$. Note that in Ref. 4a and subsequent work by these workers, all k_z's are implicitly reduced from the extended-slab-adapted BZ to the reduced-slab-adapted zone scheme.

[5]Since the $\bar{\Gamma}$ projection comes from bands which lie along a 3D symmetry axis, it would be helpful to the reader to inspect the bands calculated by B. Segall, Phys. Rev. 124, 1797 (1961). Except for a shift in the zero of energy these bands are practically identical to ours.

[6]All the degeneracies that occur for the (110) projection are between different one-dimensional representations of the group of the two-dimensional wave vector. Therefore, they are a consequence of the 3D symmetry and are progressively split as films become thinner. The degeneracy along $\bar{C}$ (including $\bar{Y}$ and $\bar{S}$) where $\bar{C}=(2\pi/a)(k_z-\alpha,\ k_z+\alpha,\ \frac{1}{2})$ occur because $(\beta-\alpha,\beta+\alpha,\ \frac{1}{2})$ differs by a (1,1,1) reciprocal-lattice vector from $(\beta-1-\alpha,\ \beta-1+\alpha,\ -\frac{1}{2})$. Although these are different points in the 3D slab-adapted BZ, they are the same point in the ordinary 3D BZ. $(\beta-1-\alpha,\ \beta-1+\alpha,\ -\frac{1}{2})$ then goes into $(1-\beta-\alpha,\ 1-\beta+\alpha,\ \frac{1}{2})$ under a twofold rotation about the $[\bar{1}10]$ axis, a symmetry operation in 3D.

[7]The degeneracy at $\bar{D}=(2\pi/a)(k_z-\frac{1}{2},\ k_z+\frac{1}{2},\ \alpha)$ between states with $k_z=\beta$ and $k_z=1-\beta$ occurs because $(\frac{1}{2}-\beta,\ \frac{3}{2}-\beta,\ \alpha)$ differs by a (0,2,0) reciprocal-lattice vector from $(\frac{1}{2}-\beta,\ -\frac{1}{2}-\beta,\ \alpha)$ which goes into $(\beta-\frac{1}{2},\ \beta+\frac{1}{2},\ \alpha)$ under a twofold rotation about the [001] axis.

[8]A. O. E. Animalu and V. Heine, Philos. Mag. 12, 1249 (1965).

[9]N. D. Lang and W. Kohn, Phys. Rev. B 1, 4555 (1970).

[10]The decay constant is a very complicated function of the potential. For an analytic expression derived from a discontinuous potential, see L. Kleinman, Phys. Rev. B 6, 1142 (1972). But in a qualitative way the decay constant is proportional to the energy difference between the surface state and the bulk bands.

[11]D. Schoenberg, in *Progress in Low Temperature Physics*, edited by C. J. Gorter (North-Holland, Amsterdam, 1957), Vol. II.

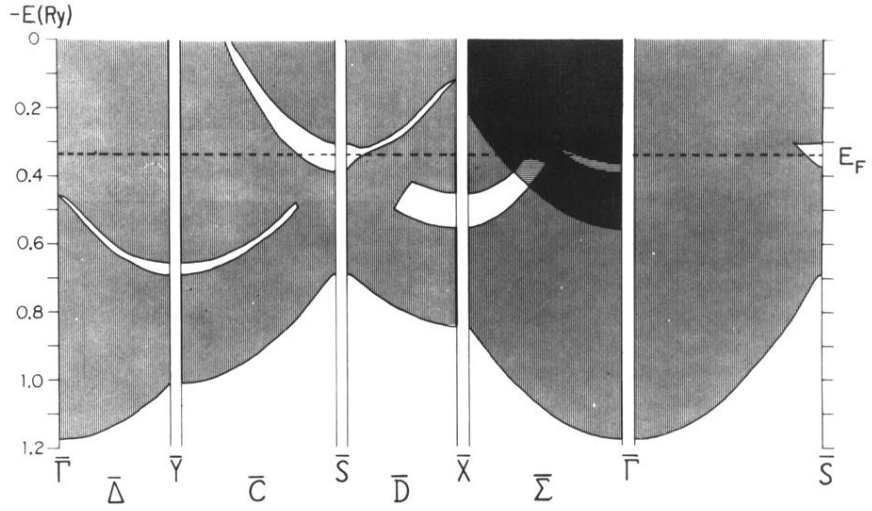

FIG. 3. Two-dimensional projection of the three-dimensional energy bands onto the (110) face. $E_F = -0.33$ Ry.